scientific reports

Check for updates

OPEN

Assessment of individual retinal layer thickness and vascular changes in Alzheimer's disease

Przemyslaw Zabel[1,2,3]✉, Anna Przekoracka-Krawczyk[4], Damian Jaworski[3,5], Katarzyna Zabel[1,2,3], Karolina Suwala[1,3], Martyna Gebska-Toloczko[1], Robert Kucharski[6] & Jakub J. Kaluzny[1,3]

Alzheimer's disease (AD) is a leading cause of dementia, underscoring the need for early and accurate diagnostic methods. This cross-sectional study examines the thickness of individual retinal layers and vessel density (VD) in 23 patients with AD and 22 healthy controls (HC). All participants underwent comprehensive ophthalmologic assessments and cognitive evaluations. AD patients exhibited significantly reduced mean macular retinal thickness compared to HC in foveal and parafoveal areas ($p < 0.05$). The most significant differences were noted in specific sectors of the Inner Nuclear Layer (INL) and Outer Nuclear Layer (ONL) ($p < 0.05$), while no significant changes were found in the Outer Retinal Layer ($p > 0.05$). Additionally, AD patients showed decreased VD in the deep vascular plexus (DVP) ($p = 0.030$) and an increased foveal avascular zone (FAZ) ($p = 0.021$). The areas under the receiver operating characteristic curves (AUC) analysis revealed the highest diagnostic accuracy for ONL thickness in the S2 sector (0.79) and for mean macular thickness in C0 and T1 sectors (0.76). Positive correlations were observed in some areas between individual retinal layers and VD in their corresponding vascular plexuses in the AD group. The findings suggest that alterations in retinal layer thickness and VD may serve as potential non-invasive diagnostic markers for AD.

Keywords Alzheimer's disease (AD), Retinal layer thickness, Vessel density (VD), Optical coherence tomography (OCT), Deep vascular plexus (DVP), Diagnostic markers

Alzheimer's disease (AD) is a chronic neurodegenerative disorder and the most common cause of dementia among the elderly[1]. First identified in the early 20th century, it remains without an effective treatment, highlighting the need for early detection and accurate diagnosis to slow the progression of neurodegenerative processes[2,3].

In 2018, the National Institute on Aging and the Alzheimer's Association (NIA-AA) revised the diagnostic framework for AD, proposing a biomarker classification system known as A/T/N. This system integrates three types of biomarkers, β-amyloid (Aβ) accumulation, pathological tau (T), and neurodegeneration or neuronal injury markers (N), to enhance diagnostic accuracy[4]. Notably, these biomarkers may show abnormalities in the preclinical phase of AD, which precedes the onset of behavioral symptoms[5]. Current diagnostic methods—such as positron emission tomography (PET), tau-PET, and lumbar puncture for assessing Aβ or tau levels in cerebrospinal fluid—are frequently expensive, invasive, and time-consuming[6,7]. These limitations drive the search for alternative diagnostic strategies that confirm AD faster and less invasively.

The interconnection between the brain and the retina has significant implications for the diagnosis of neurodegenerative diseases, including AD[8]. The accumulation of Aβ in the retina may serve as an early indicator of brain pathology. Retinal ganglion cells (RGC), which contribute to the optic nerve, are known to transport amyloid precursor protein, suggesting that retinal changes may reflect underlying brain processes[9]. This relationship opens avenues for the development of non-invasive diagnostic methods that may facilitate early detection of neurodegenerative diseases through retinal assessment. Moreover, understanding this relationship may pave the way for new therapeutic options for diseases affecting the nervous system.

[1]Department of Sensory Organ Studies, Collegium Medicum, Nicolaus Copernicus University, Sandomierska 16, Bydgoszcz 85-830, Poland. [2]Department of Ophthalmology, Collegium Medicum, Nicolaus Copernicus University, Bydgoszcz, Poland. [3]Oftalmika Eye Hospital, Bydgoszcz, Poland. [4]Laboratory of Vision Science and Optometry, Faculty of Physics and Astronomy, Adam Mickiewicz University, Poznan, Poland. [5]Division of Ophthalmology and Optometry, Department of Ophthalmology, Collegium Medicum, Nicolaus Copernicus University, Bydgoszcz, Poland. [6]Propsyche Medical Center, Bydgoszcz, Poland. ✉email: przemo.zab@gmail.com

Since the introduction of optical coherence tomography (OCT) in the 1990s, measurements of the peripapillary retinal nerve fiber layer (pRNFL) thickness has become a widely accepted parameter in the diagnosis and monitoring of various conditions, especially those affecting the optic nerve, such as glaucoma[10,11]. In particular, thinning of the pRNFL and the ganglion cell layer (GCL) due to retinal ganglion cells (RGC) damage has been observed in neurodegenerative diseases, including Parkinson's disease[12], multiple sclerosis[13], dementia with Lewy bodies[14], and especially AD[15].

OCT angiography (OCTA) extends the capabilities of OCT by providing a non-invasive method for both quantitative and qualitative assessment of vascular status in the macula and optic nerve head (ONH). Postmortem studies of AD patients have shown that neuronal apoptosis in the central nervous system correlates with vascular changes, specifically amyloid angiopathy[16]. These pathological alterations affect not only neuronal cells but also the vascular system, highlighting the potential of OCTA as a valuable diagnostic tool for AD[17].

Recent studies using spectral-domain OCT (SD-OCT) have identified significant changes in retinal thickness surrounding the macula, particularly in specific layers such as the pRNFL and the ganglion cell layer (GCL)[18,19]. Additionally, a decrease in vascular density (VD), particularly in the deep vascular plexus (DVP), has been documented through OCTA[20]. However, the individual retinal layers with the most pronounced thickness changes have not been thoroughly investigated.

The aim of this study was to investigate the thickness of individual retinal layers in the macula and analyze the correlations between these measurements and vascular density in the corresponding superficial vascular plexus (SVP) and DVP among patients with AD. Additionally, the study evaluated the diagnostic capability of these measurements—including both retinal layer thickness and VD—in discriminating AD from a healthy control group (HC).

Results

Nine eyes were initially excluded from the analyses due to poor image quality caused by vitreous floaters, motion artifacts, and incorrect segmentation in OCTA or SD-OCT examinations. A total of 55 eyes were included in the final evaluation and statistical analyses, comprising 23 eyes from the AD group and 22 eyes from the HC group. No significant differences in age, gender, or BCVA (best corrected visual acuity) were observed between the groups ($p < 0.05$). The AD group exhibited a significantly lower MMSE (mini-mental state examination) score compared to the HC group ($p < 0.001$). The demographic and clinical characteristics are presented in Table 1.

Macular retinal thickness

In the analysis of the macular retina, patients with AD showed a significant reduction in mean macular thickness compared to HC participants. The most notable differences between the study groups were found in the following areas: C0 ($p = 0.003$), T1 ($p = 0.03$), N1 ($p = 0.09$), I1 ($p = 0.014$), and S1 ($p = 0.038$). No significant differences were observed in the perifoveal area across any of the assessed quadrants ($p > 0.05$). Regarding the inner retinal layer (IRL) thickness, significant changes were noted between the examined groups, except for two sectors: S2 ($p = 0.363$) and N2 ($p = 0.195$). The largest differences occurred in the C0 sector ($p = 0.003$) and the T1 sector ($p = 0.005$). In contrast, the outer retinal layer (ORL) values were comparable between the AD and HC groups across all examined sectors ($p > 0.05$) (Table 2).

Individual macular layer thicknesses in segmentation analysis

Thickness values for all individual layers across the 9 Early Treatment Diabetic Retinopathy Study (ETDRS) sectors were obtained and are presented in Table 3. The most significant differences between the studied groups were observed in the inner nuclear layer (INL) for the following sectors: C0, S1, T1, I1, N1, and I2, as well as in the outer nuclear layer (ONL) for sectors C0, S1, T1, S2, and T2 ($p < 0.39$). Significant changes were also noted in the inner plexiform layer (IPL) only in sectors C0 and T2 ($p < 0.048$), as well as in the macular RNFL (mRNFL) and GCL in sector C0 ($p < 0.039$). Insignificant differences in thickness for the entire analyzed area between studied groups were observed in the OPL ($p > 0.05$). The most frequent changes were observed in the C0 sector across each analyzed layer (excluding the OPL); however, the most significant change was observed in the T2 sector of the ONL ($p < 0.001$).

Parameter	AD	HC	*p* value
Number of eyes (patients)	23(23)	22(22)	
Age (years)	74(64–87)*	71(64–84)*	0.690
Male/Female (%)	38.5/61.5	36.4/63.6	0.369
BCVA (logMAR)	0.0(0.0-0.096)*	0.0(0.0-0.096)*	0.504
MMSE (points)	21(16–26)*	29(27–30)*	**< 0.001**
SQ (points)	8(6–10)	8(6–9)	0.520
Q score (points)	32(27–37)	30.5(26–38)	0.436

Table 1. Demographic and clinical data. *Median (minimum and maximum values). Statistical significance was assessed using the Mann-Whitney U Test. Significant values appear in boldface. *AD* Alzheimer's Disease, *HC* healthy control, *BCVA* best corrected visual acuity, *MMSE* mini-mental state examination, *SQ* scan quality obtained from the Avanti RTVue XR device, *Q score* quality score obtained from the Heidelberg Spectralis device.

Parameter	AD					HC					*p* value
	Median	Min	Max	Q1	Q2	Median	Min	Max	Q1	Q2	
Macular retina (µm)											
C0	262	213	295	253	278	284	256	312	267	294	**0.003**
S1	339	299	371	317	342	342	321	362	336	350	**0.038**
T1	322	279	337	309	328	330	310	349	325	336	**0.003**
I1	334	293	387	321	336	341	317	362	332	347	**0.014**
N1	337	295	394	320	341	343	324	364	336	349	**0.009**
S2	295	257	331	280	301	295	270	324	286	303	0.364
T2	278	250	293	268	288	285	260	303	276	290	0.059
I2	279	244	318	262	288	288	267	312	277	294	0.091
N2	307	275	330	303	312	310	281	338	299	316	0.358
Inner retinal layers (µm)											
C0	178	132	211	165	192	199	174	225	181	206	**0.003**
S1	256	219	292	234	262	262	246	283	254	270	**0.015**
T1	243	201	258	226	248	252	233	270	245	257	**0.005**
I1	254	217	308	240	258	261	237	284	253	265	**0.013**
N1	256	216	315	234	262	261	244	285	256	268	**0.013**
S2	218	181	254	202	222	218	199	247	210	225	0.363
T2	198	172	216	190	207	207	189	224	200	212	**0.016**
I2	201	169	241	191	211	210	193	235	202	218	**0.019**
N2	228	195	253	213	234	232	213	260	221	239	0.195
Outer retinal layers (µm)											
C0	86	81	91	84	89	86	77	95	83	88	0.991
S1	80	75	91	79	82	80	75	85	78	82	0.437
T1	80	75	88	79	81	80	75	87	77	82	0.677
I1	79	74	85	78	81	80	74	86	77	81	0.955
N1	81	76	88	79	82	81	76	86	79	82	0.902
S2	78	71	83	76	80	79	73	83	77	80	0.848
T2	78	73	83	77	79	77	73	81	76	79	0.597
I2	76	70	82	74	78	77	72	80	74	78	0.744
N2	78	72	88	76	79	78	73	81	77	79	0.991

Table 2. Analysis of macular retinal thickness. Statistical significance was assessed using the Mann-Whitney U Test. Significant values appear in boldface. *AD* Alzheimer's disease, *HC* healthy control, *Min* minimum, *Max* maximum, *Q1* lower quartile, *Q2* upper quartile, *C0* central foveal thickness, *S1* inner superior, *N1* inner nasal, *I1* inner inferior, *T1* inner temporal, *S2* outer superior, *N2* outer nasal, *I2* outer inferior, *T2* outer temporal.

Vessel density in the macular area

The AD group showed a decreased VD in the macular area compared to the HC group, along with an increased foveal avascular zone (FAZ) ($p = 0.021$). Significant changes in VD were observed in the DVP of the whole enface image ($p = 0.030$), as well as in the fovea ($p = 0.004$) and the perifoveal area ($p = 0.012$). Although no statistically significant changes were identified in SVP, the p-value for SVP in the fovea approached the significance threshold ($p = 0.05$) (Table 4).

Areas under the receiver operating characteristic curves

The areas under the receiver operating characteristic curves (AUC) were calculated to evaluate the diagnostic capacity of these results in discriminating between AD and HC using the parameters with the most significant differences (AUC > 0.7). The highest AUC for individual macular layer thicknesses in the segmentation analysis were 0.79 (0.65–0.93) for the ONL in the S2 sector, 0.76 (0.62–0.88) for mean macular retinal thickness in the C0 sector, and 0.76 (0.62–0.90) in the T1 sector. For VD in individual plexuses, a value of 0.75 (0.61–0.89) was obtained for the foveal DVP (Fig. 1) (Supplementary Table 1).

Spearman correlations

Table 5 presents the Spearman correlations between VD and the thickness of the corresponding retinal layers across the same study areas. For this analysis, VD in the SVP was correlated with the thickness of the retinal layers between the ILM and the outer boundary of the IPL, while VD in the DVP was correlated with the thickness of the retinal layers between the INL and the outer boundary of the OPL. Positive correlations were observed between the ILM-IPL in the foveal area and the VD measured in the corresponding SVP ($R = 0.421$; $p = 0.005$), between the INL-OPL in the foveal area and the VD measured in the corresponding DVP ($R = 0.396$;

	AD					HC					
Parameter	Median	Min	Max	Q1	Q2	Median	Min	Max	Q1	Q2	*p* value
Retinal nerve fiber layer (μm)											
C0	11	5	18	10	14	13	10	16	12	14	**0.038**
S1	23	19	43	20	27	24	18	34	22	26	0.437
T1	17	15	31	17	18	18	16	21	16	19	0.907
I1	24	20	33	22	27	25	19	32	22	27	0.855
N1	21	18	35	18	23	21	18	26	20	22	0.654
S2	40	29	83	36	43	38	29	54	35	42	0.419
T2	20	17	31	19	21	20	17	25	19	22	0.627
I2	39	25	52	32	42	40	30	54	35	44	0.363
N2	46	35	75	43	54	49	34	63	46	53	0.339
Ganglion cell layer (μm)											
C0	12	8	20	10	16	15	11	24	13	19	**0.025**
S1	51	35	55	45	53	52	37	60	49	54	0.326
T1	45	31	56	38	48	47	35	56	42	51	0.155
I1	51	40	61	45	54	52	39	61	46	56	0.387
N1	50	38	62	41	51	50	36	58	47	54	0.321
S2	34	24	39	31	36	33	26	42	32	37	0.991
T2	33	19	46	31	38	35	28	46	32	38	0.538
I2	33	22	40	28	35	33	27	40	31	34	0.553
N2	37	29	41	32	39	36	30	44	34	39	0.991
Inner plexiform layer (μm)											
C0	19	14	27	17	21	22	17	28	19	24	**0.047**
S1	41	31	45	36	43	41	37	49	38	44	0.278
T1	40	31	44	37	42	42	35	45	39	43	0.110
I1	40	34	53	37	42	41	32	47	38	43	0.465
N1	41	34	62	37	43	42	36	47	40	43	0.479
S2	27	22	31	24	29	27	21	33	26	29	0.783
T2	31	23	35	29	33	33	29	38	31	34	**0.035**
I2	26	20	36	24	28	27	21	32	25	28	0.530
N2	28	22	31	25	30	27	24	34	26	31	0.529
Inner nuclear layer (μm)											
C0	20	13	29	17	22	23	14	31	19	26	**0.027**
S1	41	34	44	39	42	43	37	50	40	46	**0.029**
T1	37	26	42	33	41	39	33	45	38	42	**0.008**
I1	39	32	47	36	43	43	36	53	41	48	**0.015**
N1	39	34	46	36	43	44	38	50	41	46	**0.004**
S2	30	28	35	29	31	31	29	43	30	33	0.196
T2	32	28	36	30	34	33	30	38	32	35	0.071
I2	30	26	45	28	32	32	29	36	30	33	**0.036**
N2	33	30	37	31	34	33	30	38	32	35	0.124
Outer plexiform layer (μm)											
C0	24	15	44	22	29	27	20	44	25	30	0.124
S1	33	26	52	29	39	31	27	51	28	36	0.399
T1	30	24	41	27	32	31	23	40	27	32	0.954
I1	34	24	53	28	38	35	26	53	31	38	0.473
N1	34	26	62	30	40	35	25	57	28	38	0.964
S2	27	24	33	25	28	26	23	32	25	27	0.389
T2	28	24	30	26	29	26	24	30	26	28	0.554
I2	27	23	33	25	29	28	24	34	26	29	0.286
N2	29	25	37	27	31	29	25	41	27	30	0.936
Outer nuclear layer (μm)											
C0	91	70	110	80	97	96	80	108	91	105	**0.015**
S1	65	35	76	56	71	71	50	78	64	76	**0.038**
T1	71	57	82	64	72	77	46	94	73	80	**0.005**
I1	62	39	83	54	67	63	44	93	56	74	0.388

Continued

Parameter	AD					HC					*p* value
	Median	Min	Max	Q1	Q2	Median	Min	Max	Q1	Q2	
N1	65	47	81	56	72	71	44	89	65	76	0.122
S2	54	45	63	50	58	62	45	69	57	65	**0.001**
T2	53	42	62	50	55	59	43	68	53	63	**0.007**
I2	47	41	56	42	51	49	39	61	46	57	0.122
N2	52	41	65	46	55	52	43	67	51	60	0.101

Table 3. Individual macular layer thicknesses in segmentation analysis. Statistical significance was assessed using the Mann-Whitney U Test. Significant values appear in boldface. *AD* Alzheimer's disease, *HC* healthy control, *Min* minimum, *Max* maximum, *Q1* lower quartile, *Q2* upper quartile, *C0* central foveal thickness, *S1* inner superior, *N1* inner nasal, *I1* inner inferior, *T1* inner temporal, *S2* outer superior, *N2* outer nasal, *I2* outer inferior, *T2* outer temporal.

Parameter	AD					HC					*p* value
	Median	Min	Max	Q1	Q2	Median	Min	Max	Q1	Q2	
Vessel density											
SVP whole (%)	48	39	56	43	49	49	41	55	45	51	0.149
SVP fovea (%)	19	8	31	15	24	22	14	38	20	26	0.050
SVP parafovea (%)	50	36	59	45	53	52	39	58	49	54	0.224
SVP perifovea (%)	48	39	55	44	50	49	42	56	46	52	0.078
DVP whole (%)	46	37	54	40	49	49	39	64	45	51	**0.030**
DVP fovea (%)	35	21	46	30	38	40	28	48	37	43	**0.004**
DVP parafovea (%)	52	43	58	49	56	53	47	62	51	54	0.625
DVP perifovea (%)	45	36	55	40	50	50	40	65	47	52	**0.012**
FAZ (mm^2)	0.3	0.1	0.5	0.2	0.4	0.2	0.1	0.5	0.2	0.3	**0.021**

Table 4. Retinal vessel density in optical coherence tomography angiography among study groups. Statistical significance was assessed using the Mann-Whitney U Test. Significant values appear in boldface. *AD* Alzheimer's disease, *HC* healthy control, *Min* minimum, *Max* maximum, *Q1* lower quartile, *Q2* upper quartile, *SVP* superficial vascular plexus, *DVP* deep vascular plexus, *FAZ* foveal avascular zone.

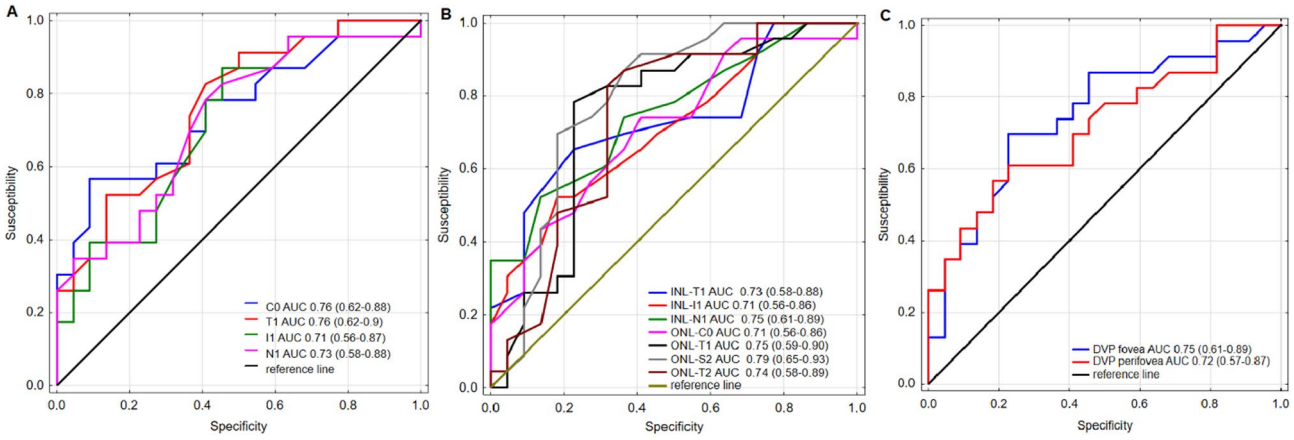

Fig. 1. Areas under the receiver operating characteristic curves for differentiating between Alzheimer's disease patients and healthy control subjects. (**A**) Mean macular retinal thickness. (**B**) Individual macular layer thicknesses in the segmentation analysis. (**C**) vessel density in the deep vascular plexus.

Parameter		Spearman coefficients	
		R value	p value
ILM-IPL fovea	SVP fovea	**0.421**	**0.005**
ILM-IPL parafovea	SVP parafovea	0.243	0.107
ILM-IPL perifovea	SVP perifovea	**0.388**	**0.008**
INL-ONL fovea	DVP fovea	**0.396**	**0.007**
INL-ONL parafovea	DVP parafovea	0.241	0.111
INL-ONL perifovea	DVP perifovea	0.221	0.145

Table 5. Spearman correlations between retinal layer thickness and vessel density in the study groups. Relationship was assessed using the Spearman Rang Order Correlations Test. Significant values appear in boldface. *ILM* internal limiting membrane, *IPL* inner plexiform layer, *ONL* outer nuclear layer, *SVP* superficial vascular plexus, *DVP* deep vascular plexus.

$p = 0.007$), and between the ILM-IPL in the perifoveal area and the VD measured in the corresponding SVP ($R = 0.388$; $p = 0.008$).

Discussion

The results of our study offer valuable insights into the thickness of individual retinal layers and vascular changes in the macula, highlighting their potential as diagnostic markers for AD. Although some studies have investigated the thickness of retinal layers in the macula of patients with AD, further research is necessary to assess individual retinal layers and their corresponding vascular plexus.

The strength of this study comes from its focus on the analysis of individual retinal layers in the macula, allowing for a precise assessment of areas affected by pathological processes in eyes with AD. In our previous study utilizing the Avanti SD-OCT device, we demonstrated that the most significant changes in retinal thickness in AD patients were observed in the ORL, which extend from the INL to the outer RPE[18] Building on this knowledge, our current study employing Spectralis SD-OCT technology reveals that the most pronounced changes occur in the INL and ONL, reinforcing our earlier observations that classified the retina solely into IRL and ORL. Additionally, we quantitatively assessed VD in specific macular regions by analyzing both the SVP and the DVP. This approach enabled us to correlate the thickness of individual retinal layers with their corresponding vascular plexuses in specific areas of the macula.

We confirmed that AD patients have a thinner mean retinal thickness in the macula compared to the HC group, and the greatest differences were observed in the central retinal thickness (C0) and in individual sectors (T1, S1, I1, N1) where the highest number of retinal ganglion cells (RGCs) are located. The changes in the retina may reflect the underlying neurodegenerative processes associated with AD. These results are consistent with previous studies that have indicated RGCs degeneration as an important marker of AD pathology[21,22].

The degeneration of ganglion cells and their axonal and dendritic projections to the retina may be the result of premature apoptotic processes, probably related to the accumulation of Aβ and tau proteins[23,24]. As AD progresses, it can be assumed that the structural abnormalities of the retina, especially its IRL, are thought to reflect pathological changes occurring in the brain, which may facilitate the identification of AD in its early stages[25].

In contrast to the IRL, the results regarding the thickness of the ORL did not show significant differences between the groups ($p > 0.05$). This observation suggests that retinal changes in AD patients may be more pronounced in the IRL, reflecting more advanced degenerative processes. Such differences may be consistent with other studies that have shown that the thickness of the ORL is less sensitive to AD-related changes, in contrast to the IRL[26]. The decrease in IRL thickness may reflect more critical pathophysiological processes related to neuronal damage and degenerative dynamics in the brain[27].

Another important finding was the change in INL thickness. The mean values of the INL thickness in sectors C0, S1, T1, I1, N1, and I2 revealed significant differences between the groups, which may indicate severe damage to this layer as a result of neurodegeneration. This is particularly important as the INL is an area of the neuron in the retina that is associated with the synaptic network, which may be crucial in the context of signal transmission and overall retinal function[28,29].

An equally important finding was the change in ONL thickness. The mean values of the ONL thickness showed significant differences between the groups, indicating severe damage as a result of neurodegeneration. The ONL layer is crucial for the function of the photoreceptor cells, which are responsible for vision and image processing[29]. In the context of AD, Santos et al. suggests that the loss of the ONL may indicate retrograde transsynaptic degeneration and that changes in the thickness of this layer may be important for the overall function of the retina and its ability to process visual information[30].

In line with our findings concerning the most pronounced changes in the IRL of the retina, recent electrophysiological studies have shown impairments in the function of RGCs and subtle alterations in photoreceptors in patients with AD. Reduced amplitudes of electroretinograms (ERG) have been linked to dysfunction in the IRL particularly in RGCs, suggesting a potential loss of function that may correlate with disease severity[31,32]. These electrophysiological changes provide additional support for the hypothesis that retinal degeneration in AD may reflect the neurodegenerative processes occurring in the brain. Furthermore,

histological analyses have confirmed these findings, revealing significant loss of both RGCs and photoreceptors, as well as bipolar cells, in the retinas of individuals with AD[33]. Such histological evidence strengthens the notion that the retina can serve as a valuable window into the neurodegenerative processes affecting the central nervous system.

In addition to assessing retinal layer thickness, our study confirmed significant reductions in VD, particularly in the DVP, and an increased FAZ in patients with AD compared to HC, which is consistent with previous studies[20,34]. These findings are particularly intriguing and suggest that vascular changes may occur concomitantly with neurodegenerative changes[35]. Reduced VD and integrity may reflect underlying brain microvascular dysfunction in the brain, which has been implicated in the pathophysiology of AD. Vascular dysregulation, characterized by amyloid angiopathy and neuronal cell death, may contribute to the progressive nature of AD[36,37]. Previous studies have emphasized the importance of ocular perfusion in maintaining retinal and nerve fibre health, and our results support the importance of vascular assessment in diagnostic procedures for suspected AD[38,39].

Spearman correlation results reveal positive associations between retinal layer thickness and VD. This suggests that structural changes in the retina may be related to the overall vascular status, underlining the importance of retinal assessment as a potential indicator of pathophysiological changes in AD. These correlations suggest a reciprocal relationship between neurodegeneration and vascular health, reinforcing the need for comprehensive assessments that include both retinal thickness and VD measurements to improve diagnostic capabilities. Such correlations may point to mechanisms that protect neuronal cells in the context of neurodegenerative diseases.

The AUC analysis confirms that retinal layer thickness and changes in VD may be useful as diagnostic biomarkers in AD. The highest AUC values were obtained for ONL thickness in the S2 sector and macular retinal thickness in the central sector, raising hopes for the use of non-invasive methods such as SD-OCT and OCTA in clinical practice.

Limitations

Despite the promising results, our study has limitations. The sample size was modest and, although we observed significant differences, future studies with larger cohorts are needed to confirm our results and to clarify the potential of these retinal markers in the clinical setting. Furthermore, longitudinal studies are necessary to clarify the relationship between changes in retinal parameters and the progression of AD symptoms over time. It is also important to consider other potential confounding factors that affect retinal morphology and vascular status. For example, changes in overall vascular health may affect retinal outcomes and need to be included in future studies. Additionally, while we acknowledge the importance of vascular and metabolic factors, the lack of detailed data on blood pressure and blood glucose levels should be recognized as a limitation.

Conclusions

In conclusion, our study demonstrates that evaluation of changes in specific layers of macular retinal thickness and VD may be significant diagnostic indicators for AD. These non-invasive measurements may improve early detection and monitoring of the disease and may be a valuable adjunct to conventional diagnostic methods. Further research is needed to understand the mechanisms behind these changes and to develop standardized protocols for incorporating retinal assessments into the clinical diagnosis of AD.

Materials and methods

Study subjects

This cross-sectional study was conducted from 2017 to 2022 at the Oftalmika Eye Hospital in Bydgoszcz, Poland. The protocol of the study was approved by the Bioethical Commission of Nicolaus Copernicus University in Torun, Collegium Medicum in Bydgoszcz, and all participants provided signed informed consent. The study was conducted in accordance with the Helsinki Declaration, and participants were fully informed about the nature of the study and its potential consequences before providing their consent.

Each individual included in the study underwent a cognitive function assessment by a psychologist using the MMSE screening test. All patients underwent a comprehensive ophthalmological examination, including measurement of BCVA with Snellen charts, tonometry (Icare TAO1i, Finland Oy, Vantaa, Finland), fundus evaluation with a Volk lens, biomicroscopy, measurement of retinal structures using SD-OCT, and evaluation of VD with OCTA. The visual acuity measured with Snellen charts was subsequently converted into the logarithm of the minimum angle of resolution (logMAR) for statistical analysis. These examinations were conducted by an ophthalmologist in a single session.

A group of AD patients were referred from the Center for Psychoneurology of the Elderly in Bydgoszcz and the Department of Psychiatry of the Collegium Medicum of the Nicolaus Copernicus University in Bydgoszcz. A diagnosis of AD was made by a psychiatrist based on the guidelines of the National Institute on Aging and the Alzheimer's Association and the criteria of the Diagnostic and Statistical Manual of Mental Disorders (DSM-IV). The diagnosis was confirmed by neuroimaging, which showed the presence of amyloid plaques in the brain using positron emission tomography (PET) with the radioligand Florbetapir (18 F). Patients were classified as amyloid-positive if their neocortex standardized uptake value ratio was greater than 1.5. Patients with mild to moderate dementia (MMSE scores between 10 and 23) were eligible for inclusion in the study. Other criteria included normal intraocular pressure (IOP) ≤ 21 mmHg and the absence of fundus changes suggestive of retinal or optic nerve diseases (e.g., AMD or glaucoma).

Members of the Senior Club in Bydgoszcz formed the HC group. After giving their consent, they underwent comprehensive ophthalmological and psychological assessments. To be included in the control group, participants had to have a normal MMSE score (≥ 27 points), no evidence of any eye or neurodegenerative diseases.

Exclusion criteria included those younger than 55 years or older than 87 years, those with BCVA less than 0.6, refractive errors greater than +3.0 Dsph or less than −3.0 Dsph, and a history of eye surgery other than uncomplicated cataract phacoemulsification. The study also excluded individuals with any eye diseases (defined as those identified through a comprehensive ophthalmological examination, SD-OCT assessment, and patient interview) or neurodegenerative diseases (except for Alzheimer's disease confirmed by PET scan), which were defined based on psychological assessment and patient interview. Additionally, individuals with a history of head or eye trauma, increased IOP (>21 mmHg), diabetes, uncontrolled hypertension (greater than 150/90 mm Hg), obesity (body mass index over 30 kg/m^2), and smoking were excluded from the study.

Optical coherence tomography angiography

OCTA imaging was conducted using the Avanti RTVue XR (Optovue, Inc., Fremont, CA, USA), which scans at a rate of 70.000 A-scans per second and provides an axial resolution of 5 µm with a light source wavelength of 840 ± 10 nm. A system (software version 2017.1.0.151) with featuring three-dimensional Projection Artifact Removal (3D PAR) was used, which effectively reduces projection artifacts in all deeper layers while preserving their authentic layout and improving the FAZ parameters.

The macula was analyzed using B-scans covering a area of 6 × 6 mm^2, scanned both vertically and horizontally. Each B-scan consisted of 400 A-scans centered on the fixation point. Macular VD was assessed across the 6.0 × 6.0 mm^2 area, within the 1-mm diameter foveal annulus, the parafoveal area between the 1-mm and 3-mm annuli, and the perifoveal area. Data were processed using commercial software that automatically segmented the SVP and DVP and measured the VD in both plexuses. The SVP comprised the area between the ILM and the outer boundary of the IPL, while the DVP comprised the area between the outer boundary of the IPL and the outer boundary of the OPL.

Both eyes of all participants were examined on the same day between 8:00 AM and 12:00 PM following pupil dilation. Only measurements of high technical standard, with a scan quality (SQ) of 6 or above on a 10-point scale (as indicated by the commercial camera), were included in further analysis. Measurements showing motion artifacts on the en face images, such as irregular vessel patterns or blurred images, were excluded.

Spectral-domain optical coherence tomography

The retinal structure analysis was conducted using the Spectralis SD-OCT device (Heidelberg Engineering GmbH, Heidelberg, Germany), equipped with real-time eye-tracking software (Heidelberg Eye Explorer, version 1.10.4.0). Each participant was scanned in IR + OCT mode with a 30° area setting. The acquired volumes consisted of 61 images, each measuring of 768 × 496 pixels (width × height). The axial resolution was 3.9 microns, and the transversal resolution ranged from 10 to 12 microns. Importantly, high-resolution (HR) scans were utilized to ensure optimal image clarity and precision. The spacing between B-scans varied from 120 to 140 microns. To reduce speckle noise and improve image contrast, each B-scan was averaged from five aligned images using TruTrack active eye tracking technology.

The Spectralis software provided thickness measurements for several retinal layers, including: (1) mean macular retinal thickness, (2) mRNFL, (3) GCL, (4) IPL, (5) INL, (6) OPL, (7) ONL, (8) retinal pigment epithelium (RPE), (9) IRL—defined as the area from the ILM to the external limiting membrane (ELM), and (10) ORL—defined as the area from the ELM to Bruch's membrane (Fig. 2).

After the automatic segmentation of each slice, the Spectralis software provides thickness maps divided into nine subfields as defined by the ETDRS. Inner, intermediate, and outer rings with diameters of 1, 3, and 6 mm respectively, were considered for the analysis. The average of all points within the inner 1-mm radius circle was defined as central foveal thickness (C0). The intermediate ring was divided into four sectors designated as inner superior (S1), inner nasal (N1), inner inferior (I1), and inner temporal (T1); and so was the outer ring, with four sectors designated as outer superior (S2), outer nasal (N2), outer inferior (I2), and outer temporal (T2). The numerical values recorded for each of the nine zones for every layer were used in the analysis.

The same experienced operator performed all scans, and no manual correction was applied to the SD-OCT output. The quality of the scans was assessed on a scale ranging from 0 (poor) to 40 (high), and scans scoring lower than 25, as well as those exhibiting incorrect segmentation, were discarded.

Statistical analysis

Statistical analyses were performed using Statistica Software (ver. 14; TIBCO Software Inc.). First of all, the data were compared between the eyes as no significant difference was found, further analyses were performed on the one eye (the right eye) of each participant. The Shapiro-Wilk test showed that the data sets were far from a normal distribution, so nonparametric tests were used for farther analyses. The median, minimum (Min), and maximum (Max) values, along with the lower (Q1) and upper (Q2) quartiles, were calculated. Among the groups, OCTA and SD-OCT data were compared by using the Mann-Whitney U Test. Correlations between measured parameters were assessed using the Spearman rang order correlations test.

The AUC was used to determine the diagnostic accuracy of the measured parameters in discriminating between AD and HD groups. The AUC of 1.0 represents perfect discrimination, a value of 0.7 or higher represents acceptable discrimination, whereas an AUC of 0.5 represents chance discrimination. Differences were considered significant if the *p*-value was equal to 0.05 or less.

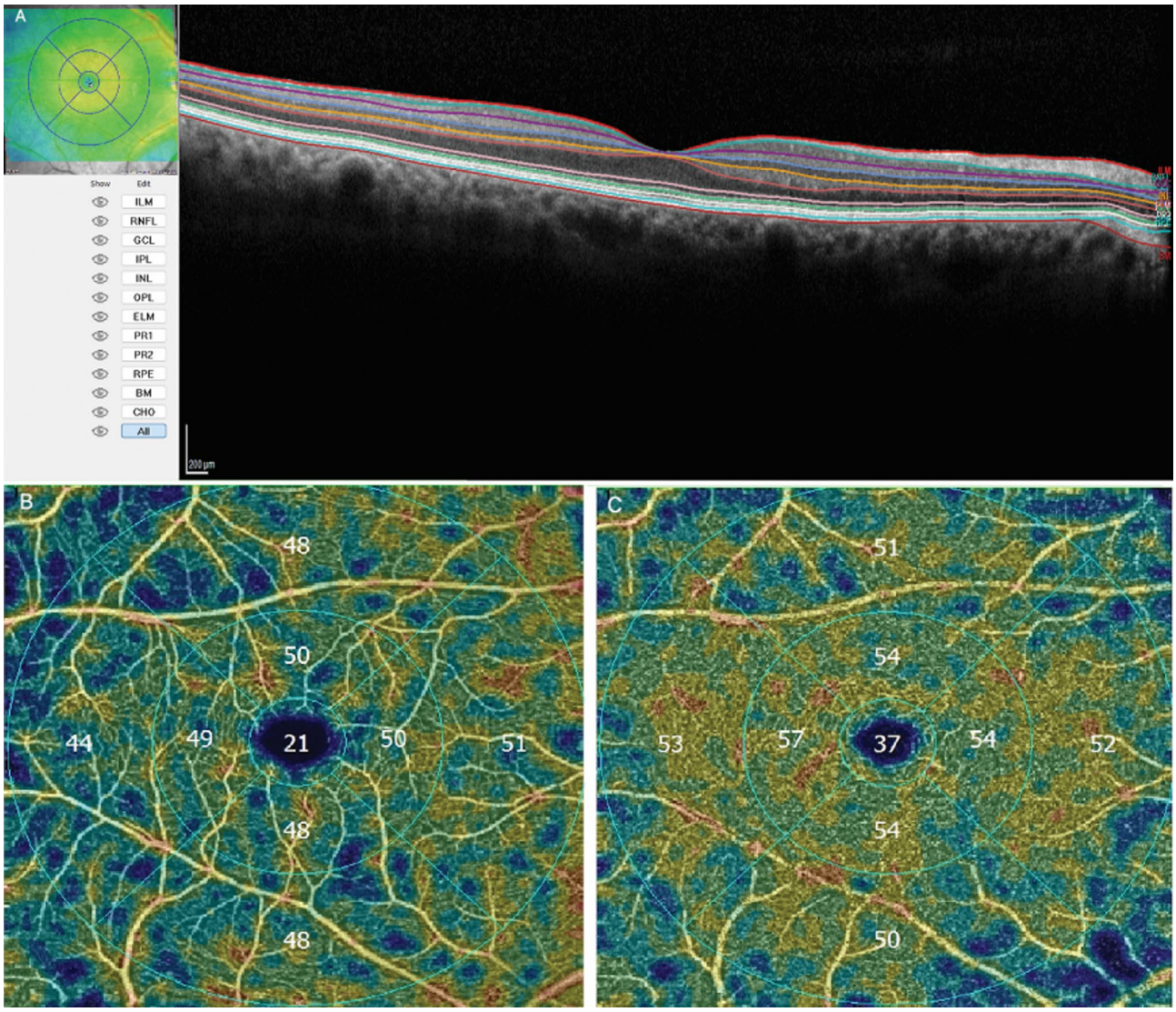

Fig. 2. Sample results of the study for the right eye of a 78-year-old patient with Alzheimer's disease. (**A**) Retinal thickness maps divided into nine subfields as defined by the Early Treatment Diabetic Retinopathy Study (ETDRS), along with retinal layer segmentation in spectral domain optical coherence tomography. Layers: internal limiting membrane (ILM), retina nerve fiber layer (RNFL), ganglion cell layer (GCL), inner plexiform layer (IPL), inner nuclear layer (INL), outer plexiform layer (OPL), external limiting membrane (ELM), photoreceptor layer (PR), retina pigment epithelium (RPE), Bruch membrane (BM). (**B**) Superficial vascular plexus with qualitative and quantitative assessments of vessel density, divided into nine subfields as defined by the ETDRS. (**C**) Deep vascular plexus with qualitative and quantitative assessments of vessel density, divided into nine subfields as defined by the ETDRS.

Data availability

The datasets used and/or analyzed during the current study are available from the corresponding author on reasonable request.

Received: 16 February 2025; Accepted: 13 May 2025
Published online: 19 May 2025

References

1. Scheltens, P. et al. Alzheimer's disease. *Lancet* **397**, 1577–1590 (2021).
2. Hippius, H. & Neundörfer, G. The discovery of Alzheimer's disease. *Dialog Clin. Neurosci.* **5**, 101–108 (2003).
3. Juganavar, A., Joshi, A. & Shegekar, T. Navigating early Alzheimer's diagnosis: a comprehensive review of diagnostic innovations. *Cureus* **15**, 9 (2023).
4. Jack, C. R. et al. NIA-AA research framework: toward a biological definition of Alzheimer's disease. *Alzheimers Dement.* **14**, 535–562 (2018).

5. Dubois, B. et al. Preclinical Alzheimer's disease: definition, natural history, and diagnostic criteria. *Alzheimers Dement.* **12**, 292–323 (2016).
6. Van Oostveen, W. M. & de Lange, E. C. Imaging techniques in Alzheimer's disease: a review of applications in early diagnosis and longitudinal monitoring. *Int. J. Mol. Sci.* **22**, 2110 (2021).
7. Brier, M. R. et al. Tau and Aβ imaging, CSF measures, and cognition in Alzheimer's disease. *Sci. Transl Med.* **8**, 338ra66 (2016).
8. Ausó, E., Gómez-Vicente, V. & Esquiva, G. Biomarkers for Alzheimer's disease early diagnosis. *J. Pers. Med.* **10**, 114 (2020).
9. Wang, L. & Mao, X. Role of retinal amyloid-β in neurodegenerative diseases: overlapping mechanisms and emerging clinical applications. *Int. J. Mol. Sci.* **22**, 2360 (2021).
10. Huang, D. et al. Optical coherence tomography. *Science* **254**, 1178–1181 (1991).
11. Bussel, I. I., Wollstein, W., Schuman, J. S. & G. & OCT for glaucoma diagnosis, screening and detection of glaucoma progression. *Br. J. Ophthalmol.* **98**, ii15–ii19 (2014).
12. Satue, M. et al. Retinal thinning and correlation with functional disability in patients with Parkinson's disease. *Br. J. Ophthalmol.* **98**, 350–355 (2014).
13. Birkeldh, U. et al. Retinal nerve fiber layer thickness associates with cognitive impairment and physical disability in multiple sclerosis. *Mult Scler. Relat. Disord.* **36**, 101414 (2019).
14. Moreno-Ramos, T. et al. Retinal nerve fiber layer thinning in dementia associated with Parkinson's disease, dementia with lewy bodies, and Alzheimer's disease. *J. Alzheimers Dis.* **34**, 659–664 (2013).
15. Blanks, J. C., Hinton, D. R., Sadun, A. A. & Miller, C. A. Retinal ganglion cell degeneration in Alzheimer's disease. *Brain Res.* **501**, 364–372 (1989).
16. Zlokovic, B. V. Neurovascular pathways to neurodegeneration in Alzheimer's disease and other disorders. *Nat. Rev. Neurosci.* **12**, 723–738 (2011).
17. Patton, N. et al. Retinal vascular image analysis as a potential screening tool for cerebrovascular disease. *J. Anat.* **206**, 318–348 (2005).
18. Zabel, P. et al. Quantitative assessment of retinal thickness and vessel density using optical coherence tomography angiography in patients with Alzheimer's disease and glaucoma. *PLoS ONE.* **16**, e0248284 (2021).
19. Mei, X. et al. Changes in retinal multilayer thickness and vascular network of patients with Alzheimer's disease. *BioMed. Eng. OnLine.* **20**, 1–13 (2021).
20. Zabel, P. et al. Comparison of retinal microvasculature in patients with Alzheimer's disease and primary open-angle glaucoma by optical coherence tomography angiography. *Investig Ophthalmol. Vis. Sci.* **60**, 3447–3455 (2019).
21. Davis, M. R. et al. Retinal ganglion cell vulnerability to pathogenic Tau in Alzheimer's disease. *BioRxiv* (2024).
22. Kim, J. I. & Kang, B. H. Decreased retinal thickness in patients with Alzheimer's disease is correlated with disease severity. *PLoS ONE.* **14**, e0224180 (2019).
23. Gupta, V. et al. One protein, multiple pathologies: multifaceted involvement of amyloid B in neurodegenerative disorders of the brain and retina. *Cell. Mol. Life Sci.* **73**, 4279–4297 (2016).
24. Gupta, V. B. et al. Retinal changes in Alzheimer's disease—integrated prospects of imaging, functional and molecular advances. *Prog Retin Eye Res.* **82**, 100899 (2021).
25. Shi, Z. et al. Retinal nerve fiber layer thickness is associated with hippocampus and lingual gyrus volumes in nondemented older adults. *Prog Neuro Psychopharmacol. Biol. Psychiatry.* **99**, 109824 (2020).
26. Cunha, L. P. et al. Macular thickness measurements with frequency domain-OCT for quantification of retinal neural loss and its correlation with cognitive impairment in Alzheimer's disease. *PLoS ONE.* **11**, e0153830 (2016).
27. Chiquita, S. et al. The retina as a window or mirror of the brain changes detected in Alzheimer's disease: critical aspects to unravel. *Mol. Neurobiol.* **56**, 5416–5435 (2019).
28. López-Cuenca, I. et al. The relationship between retinal layers and brain areas in asymptomatic first-degree relatives of sporadic forms of Alzheimer's disease: an exploratory analysis. *Alzheimers Res. Ther.* **14**, 79 (2022).
29. Robinson, E. K. et al. Retinal neurodegeneration and synaptic loss in relations to core-proteinopathies and cognitive scores in MCI and AD patients. *Alzheimers Dement.* **20**, e087799 (2025).
30. Santos, C. Y. et al. Change in retinal structural anatomy during the preclinical stage of Alzheimer's disease. *Alzheimers Dement. Diagn. Assess. Dis. Monit.* **10**, 196–209 (2018).
31. Liao, C. et al. Retinal dysfunction in Alzheimer's disease and implications for biomarkers. *Biomolecules* **11**, 1215 (2021).
32. Asanad, S. et al. Retinal ganglion cell dysfunction in preclinical Alzheimer's disease: an electrophysiologic biomarker signature. *Sci. Rep.* **11**, 6344 (2021).
33. Asanad, S. et al. The retina in Alzheimer's disease: histomorphometric analysis of an ophthalmologic biomarker. *Investig Ophthalmol. Vis. Sci.* **60**, 1491–1500 (2019).
34. Yeh, T. C. et al. Retinal microvascular changes in mild cognitive impairment and Alzheimer's disease: a systematic review, meta-analysis, and meta-regression. *Front. Aging Neurosci.* **14**, 860759 (2022).
35. Gaire, B. P. et al. Alzheimer's disease pathophysiology in the retina. *Prog Retin Eye Res.* **101**, 101273 (2024).
36. Shi, H. et al. Identification of early pericyte loss and vascular amyloidosis in Alzheimer's disease retina. *Acta Neuropathol.* **139**, 813–836 (2020).
37. Ashraf, G. et al. Retinal imaging biomarkers of Alzheimer's disease: A systematic review and meta-analysis of studies using brain amyloid beta status for case definition. *Alzheimers Dement. Diagn. Assess. Dis. Monit.* **15**, e12421 (2023).
38. Romaus-Sanjurjo, D. et al. Alzheimer's disease seen through the eye: ocular alterations and neurodegeneration. *Int. J. Mol. Sci.* **23**, 2486 (2022).
39. Cabrera DeBuc, D., Somfai, G. M. & Koller, A. Retinal microvascular network alterations: potential biomarkers of cerebrovascular and neural diseases. *Am. J. Physiol. Heart Circ. Physiol.* **312**, H201–H212 (2017).

Author contributions

Conception and design: P.Z., K.Z., J.J.K. Development of methodology: P.Z., J.J.K., R.K. Data acquisition: D.J., K.S., M.G-T. Analysis and interpretation of data: P.Z., A.P-K. Statistic Review: A.P-K. Writing, review of manuscript: all authors.

Declarations

Competing interests

The authors declare no competing interests.

Additional information

Supplementary Information The online version contains supplementary material available at https://doi.org/10.1038/s41598-025-02377-1.

Correspondence and requests for materials should be addressed to P.Z.